nature energy

Review article

https://doi.org/10.1038/s41560-025-01767-z

Stabilizing lithium-metal electrodes with polymer coatings

Received: 13 October 2024

Accepted: 21 March 2025

Published online: 14 May 2025

Check for updates

Zhuojun Huang [1,2], Hao Lyu [2], Louisa C. Greenburg[1], Yi Cui [1,3] ✉ & Zhenan Bao [2] ✉

Increasing the energy density of batteries can accelerate the deployment of electric vehicles, expand the utilization of renewable energy and, in turn, reduce greenhouse gas emissions. Different from commercially available lithium-ion batteries, high-energy-density lithium-metal batteries use metallic lithium instead of graphite as the negative electrode. The commercialization of lithium-metal batteries is hindered by the electrochemical instability of lithium metal. Polymer coatings have shown promise in addressing issues related to each step of heterogeneous lithium deposition. Here we summarize the current understanding of key design principles and highlight relevant coating compositions. Moreover, we discuss high-performing coating–electrolyte pairs and provide an outlook on interface design for novel electrolytes.

Lithium-metal batteries (LMBs) are widely regarded as the next generation of energy storage devices because of their high anode specific energy density of 3,860 Ah kg^{-1} (refs. 1,2). One of the main limitations towards the long-term stable operation of LMBs is the uncontrolled deposition of lithium (Li) metal, and key to improving the battery performance is stabilizing the deposition of Li (ref. 3). With this aim, modifications to the Li-metal electrode have been made to both the current collector and the electrode–electrolyte interface.

Modification of the current collector often entails controlling the charge transfer and/or nucleation and growth to alter the deposition of Li onto the modified current collector. For example, micro-structured carbon-based materials lowered the morphology of fibrous Li by reducing localized current densities[4]. Some metals, such as gold, form alloys with Li, and patterning these metals on the current collector alters the Li nucleation behaviour, giving a more uniform Li morphology[5].

Alternatively, one can modify the electrode–electrolyte interface directly[6]. Some researchers have explored pre-forming the solid–electrolyte interphase (SEI) before cell assembly. Li metal reacts with materials such as fluorinated carbonate solvents[7], fluoropolymers[8] or ionic liquids[9], and the reaction products were found to form mechanically robust and/or inorganic-rich SEIs. Others have modified the electrode–electrolyte interface via the direct application of a coating layer on Li. For example, interconnected carbon spheres or multilayered graphene were used to encapsulate Li whisker growth[10]. A layer of aluminium oxide (Al_2O_3) was deposited on Li via atomic layer deposition to improve the wettability of the Li electrode and promote the formation of a dense SEI[11]. However, the efficacy of these inorganic coatings may be limited by their inherent brittleness[12].

A review by Zhang, Huang and colleagues examined methods for applying inorganic and organic coatings to Li-metal electrodes for batteries with both liquid-state and solid-state electrolytes[6]. Another review by Liu, Liu and co-workers detailed the ion-conduction mechanism of polymer and inorganic coatings for Li electrodes[13]. Here we focus on polymer coatings, relating their chemical structure to their proposed mechanism of stabilizing the deposition of Li metal. Compared with inorganic materials, polymers are softer and can form a conformal interface with Li. There is a large library of different polymer chemistries that can be used to design coatings with various targeted mechanical, transport and electrochemical properties. Polymers can also be used to form composites with inorganic materials, creating more opportunities to introduce new functionalities.

First, we outline three mechanisms by which polymer coatings can improve the performance of the Li-metal anode: (1) maintaining uniform coverage to prevent pinholes; (2) homogenizing charge distribution; and (3) regulating reactions at the interface to improve the SEI chemistry. Then, for each mechanism, we show how different design

[1]Department of Materials Science and Engineering, Stanford University, Stanford, CA, USA. [2]Department of Chemical Engineering, Stanford University, Stanford, CA, USA. [3]Stanford Institute for Materials and Energy Sciences, SLAC National Accelerator Laboratory, Menlo Park, CA, USA. ✉e-mail: yicui@stanford.edu; zbao@stanford.edu

concepts are realized with distinct combinations of polymer backbones and side-chain functionalities. Finally, we discuss the performance of coating–electrolyte pairs and lay out future directions towards designing polymers for advanced electrolytes.

Protection mechanisms of polymer coatings

The uneven deposition of Li occurs because of the delicate nature of the SEI layer, which forms when Li comes into contact with the electrolyte[3]. Over time, as the Li negative electrode undergoes charging and discharging, the change in volume leads to the formation of pinholes in the SEI. Subsequently, Li is deposited more rapidly at these pinholes due to easier access of Li ions (Li^+)[14]. This uneven deposition process worsens as the number of cycles increases, ultimately resulting in a decreased battery capacity, potential short circuits and, in severe cases, battery failure (Fig. 1a).

To tackle this issue, researchers have proposed the use of polymer coatings to promote the more homogeneous deposition of Li. Figure 1a,b presents an overview of the strategies and the polymer structures and additional chemical modifications that have been used.

The first strategy involves applying a robust polymer layer that maintains coverage of the interface. Unlike the native SEI, this polymer coating may be designed to possess a high degree of toughness to maintain uniform coverage of the Li electrode. To achieve this, the polymer toughness can be enhanced via crosslinking. For example, a crosslinked layer of the organic–inorganic hybrid polymer alucone increases the mechanical strength and can be deposited directly onto the Li electrode via molecular layer deposition[12]. Alternatively, one can use crosslinking chemistries such as methacrylate-based radical crosslinking[15] or the thiol-ene click reaction[16] to strengthen the polymer matrix. A phosphate methacrylate-based crosslinked layer has been introduced atop a polyethylene oxide (PEO) coating to provide mechanical stabilization[17]. One may also use the in situ polymerization of electrolyte additives to generate a mechanically stable polymer interface (for example, polyoxymethylene (POM))[18]. In addition to covalent crosslinking, non-covalent dynamic crosslinking, such as hydrogen bonds and ionic interactions, have been used to tune the mechanical stability of polymer coatings. Ensuring an initial surface coverage may be insufficient when pinholes appear during charge–discharge cycles. These surface defects become hotspots for rapid Li deposition due to the large flux of ions through pinholes, which are locations of high electric field concentration. The dynamic nature of the polymers (as shown by having a crossover in the storage and loss rheological modulus) not only increases the toughness of the polymer but also heals pinholes, even if they form during processing. A branched polyurea (PU) coating, rich in hydrogen bonds, has demonstrated efficacy in stabilizing Li deposition[19], owing to the dynamic behaviour brought by these non-covalent interactions. Hydrogen bonding can also be deliberately incorporated into polymer backbones such as those of perfluoropolyether (PFPE)[20]. 'Silly Putty', a siloxane-based polymer containing dynamic boronic ester crosslinkers, has been investigated as a coating material[21]. Ionic interactions represent another category of non-covalent dynamic bonds. For instance, a polymer network was formed of fluorinated tetraethylene glycol (FTEG) chains and tetrahedral $Al(OR)^-$ coordination centres (where R is a soft fluorinated linker)[22]. Polyacrylic acid (PAA) was crosslinked with Li^+ to give lithiated polyacrylic acid (Li-PAA), enhancing the toughness of the polymer matrix[23]. Another approach for enhancing toughness involves blending polymers with high-modulus materials. For example, various polymers have been fortified with materials such as polyhedral oligomeric silsesquioxane (POSS)[24], lithium silicate (Li_xSiO_y)[25], lithium fluoride (LiF)[26], graphene oxide[27], Al_2O_3 (refs. 28,29) and lithium phosphorus oxynitride (LiPON)[30] to bolster their mechanical toughness.

A second mechanism for achieving an effective polymer coating is to homogenize the charge distribution. Polymer coatings can be designed to impact the ion transport and/or the reaction kinetics to improve Li-metal deposition. Several strategies have been used to control Li^+ transport with a polymer coating. A coating with pyrrolidinium cations was hypothesized to shield Li^+ from the concentrated electric fields at fast growing Li filament tips, and indeed more uniform Li deposition was observed[31]. Other approaches involved establishing dedicated ion-transport pathways within the polymer. This can be achieved using materials such as polymers of intrinsic microporosity (PIMs)[32] or polydimethylsiloxane (PDMS) with etched nanopores[33]. Alternatively, single-ion conductors such as Nafion[29], or polyether ether ketone (PEEK)[24] with sulfonate (SO_3^-) added, can also be used. Moreover, ion-conductive inorganics such as Li_3N can be added to regulate Li^+ transport[34]. Besides these methods, ion conduction can be controlled through polar interactions. This includes polymers with polar groups, such as PU[35], polyacrylonitrile (PAN)[36] or polyvinylidene fluoride (PVDF)[37]. Alternatively, polar functionalities such as zwitterion moieties[15] or inorganic compounds such as LiF[38–40] and zirconium dioxide (ZrO_2)[41] may be incorporated.

Another way to regulate the charge distribution at the interface involves tuning both the ion transport and the reaction kinetics. For instance, PFPE, which is an electronic insulator, has demonstrated the ability to decrease the reaction kinetics. When ion-conducting lithium styrene trifluoromethanesulfonyl imide (Li-STFSI) was added at a concentration of 1.5 mol kg^{-1}, the resulting polymer, when swelled in solvents, has a Li diffusion coefficient of ~10^{-6} cm^2 s^{-1}, which is similar to that of a liquid electrolyte[42]. This polymer reduced the ratio of the reaction to the ion-transport rate (that is, the Damköhler number) by more than an order of magnitude and contributed to a more uniform Li deposition morphology.

The third approach is to regulate interfacial reactions and improve the SEI chemistry. Reactive polymer coatings have been designed to partcipate directly in SEI formation. For example, PVDF[43] and poly(vinylidene fluoride-co-hexafluoropropylene) (PVDF-HFP)[44] can be reduced by Li and generate the beneficial SEI component LiF. In another study, the introduction of a ureidopyrimidinone (UPy) unit into the PEO chain can result in a chemical reaction with Li and the formation of an interfacial layer that provides improved adhesion to the electrode[45]. Various functional groups, for example, 1,3-dioxolane[46], sulfonyl fluoride[27] and alcohol[47] groups, have been incorporated into polymers such as polynorbornene (PNB) and polyethylene (PE). These reactive moieties integrate the polymer into the SEI layer while also facilitating the retention of the electrolyte at the electrode interface. Furthermore, $LiNO_3$, an additive known for promoting a uniform Li deposition morphology, has been embedded within a PVDF-HFP polymer coating to give prolonged and gradual release of $LiNO_3$ (ref. 48). Polymer coatings can also be designed to influence the SEI formation process, contributing to the development of a more robust SEI. For example, a siloxane-based polymer has been engineered with side chains that selectively transport Li salts over solvent molecules[49]. This selective transport promotes the creation of a stable SEI derived from Li salts, as opposed to the more fragile SEI derived from solvents[50]. Other than actively influencing the SEI chemistry, polymers that are more inert with Li metal than the electrolyte, such as PDMS[51] and PEO[17], may limit chemical reactions between Li and the electrolyte, and improve the electrode stability.

In the next three sections, we provide more in-depth analysis of specific design cases within each of the three outlined strategies. Our primary focus is on studies involving chemical functionalization. Unlike composite blends of commercial polymers and additives, the rational molecular design of polymer coatings provides more opportunities by which to investigate intricate structural–property relationships via chemical design.

Maintain coverage of the interface

Macroscopic mechanical property requirements

Previous theoretical studies have proposed that materials with an elastic modulus of 2 GPa and higher (that is, twice that of Li metal) may

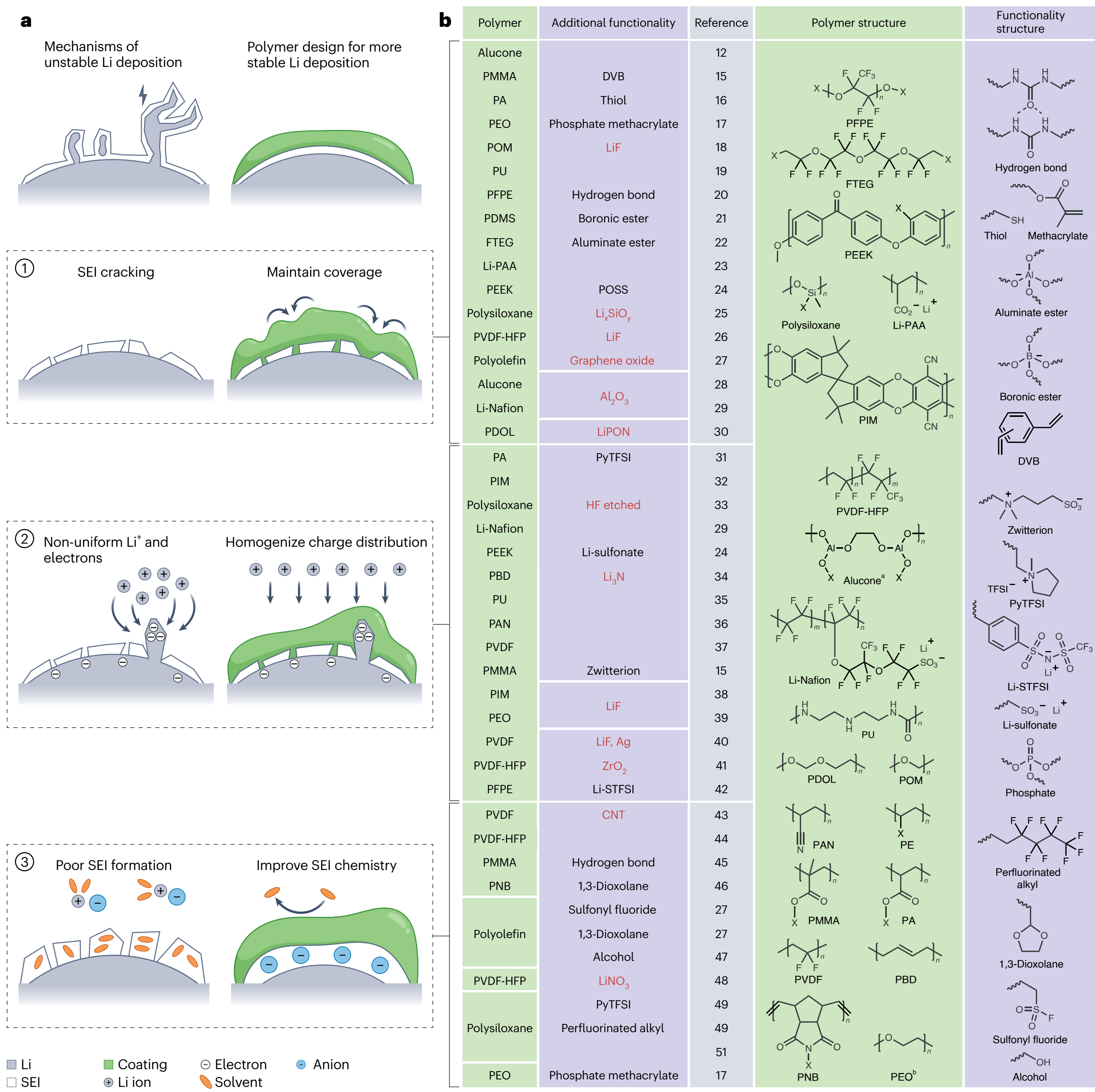

Fig. 1 | Mechanisms and chemistries of polymer coatings. a, Schematics showing the unstable Li deposition process (left) and polymer coatings that stabilize Li deposition (right) via (1) maintaining coverage to prevent pinhole formation, (2) promoting a homogeneous flux of Li^+ by modulating the charge distribution and (3) improving the SEI chemistry. **b**, Compositions of reported polymer coatings. The names and structures of polymer backbones (green) and additional functionalities (purple, if any) are listed and separated into the three mechanisms. On the polymer structure, X denotes the attachment locations of functionalities. The names of composite components or the etching process are given in red text. PFPE, perfluoropolyether; FTEG, 1H,1H,11H,11H-perfluoro-3,6,9-trioxaundecane-1,11-diol; PEEK, polyether ether ketone; PIM, polymer of intrinsic microporosity; Li-PAA, lithiated polyacrylate acid; PVDF-HFP, poly(vinylidene fluoride-co-hexafluoropropylene); PMMA, poly(methyl methacrylate); PU, polyurea; PDOL, polydioxolane; POM, polyoxymethylene; PAN, polyacrylonitrile; PA, polyacrylate; PVDF, poly(vinylidene fluoride); PBD, polybutadiene; PEO, polyethylene oxide; PNB, polynorbornene; PE, polyethylene; POSS, polyhedral oligomeric silsesquioxane; DVB, divinylbenzene; LiPON, lithium phosphorus oxy-nitride; Li-STFSI, lithium sulfonyl(trifluoromethane)sulfonimide styrene; PyTFSI, pyrrolidinium bis(trifluoromethanesulfonyl)imide; CNT, carbon nanotube. [a]Alucone is attached to the substrate through X. [b]PEO is assumed to have methyl termination throughout this review.

suppress the growth of dendritic Li (ref. 52). However, the difficulty of forming a conformal coherent interface between high-modulus materials and Li may result in non-uniform Li deposition, as shown by the fibrous growth of Li in ceramic solid-state batteries[53]. On the other hand, other investigations have shown that a soft coating layer with a modulus lower than that of Li may still reduce Li filament growth through suitable design. Helms and collaborators reported that stable Li deposition can be achieved using polymeric interfaces with a shear modulus (G_s) in the range of 165–376 MPa (ref. 38). These coatings have a low modulus compared with that of Li (G_{Li}; that is, G_s/G_{Li} is 0.023–0.09). Bao, Cui and colleagues introduced a soft (~1 MPa storage modulus at 1 Hz) and flowable polymer coating that is capable of consistently covering the electrode surface during cycling, resulting in uniform and dense Li deposition[19]. In this approach, the role of the coating is to facilitate uniform Li^+ flux and to establish a uniform and conformal interface with Li rather than suppressing Li filament protrusion.

A key design strategy is to increase the toughness of the coating. A brittle layer is prone to fracturing under stress from repeated cycling, whereas an excessively soft layer tends to disintegrate on encountering protrusions or may be damaged easily during cell assembly. One way to increase the polymer toughness is by combining both rigid and soft components (Fig. 2a). This design concept is corroborated by theoretical insights. A coarse-grained molecular dynamics study by Qin and co-workers explored the correlation between the polymer coating dynamics and the Li growth morphology, observing that an interface possessing viscoelastic mechanical properties (that is, between solid and liquid-like) promotes more uniform Li growth[54]. Increasing the toughness can be accomplished through the incorporation of inorganic additives such as POSS[24], Li_xSiO_y (ref. 25), LiF[26], graphene oxide[27], Al_2O_3 (refs. 28,29) and LiPON[30]. Alternatively, toughness can be enhanced by crosslinking the polymer with covalent or dynamic bonds. In addition to polymer coatings, polymer electrolytes with both rigid (ethylene styrene) and soft (ethylene oxide) building blocks have demonstrated promise in suppressing Li filament growth[55,56].

Other factors in designing mechanically stable interfaces on Li metal include the chemical stability, long-term stability and polymer–electrolyte interaction. Chemical stability can be improved by reducing the use of Li-reactive functional groups such as hydrogen bonds. Long-term stability can be evaluated by disassembling cells after different periods of cycling. Polymer–electrolyte interactions affect both the ionic conductivity and mechanical properties of the coating, and these properties should be reported in the swollen state.

Chemistries for tuning the coating mechanics

Depending on the crosslinking density, covalent crosslinking may increase the fracture toughness of a polymer while preserving a certain degree of polymer chain flexibility (Fig. 2b). Common crosslinking groups used in polymer coatings include thiol-ene click chemistry and acrylate- and methacrylate-based radical crosslinking (Fig. 2c). Other crosslinking chemistries may include azide and benzophenone[57]. These crosslinking reactions can be activated ex situ using ultraviolet light or heat, enabling facile processing during coating formation and application. Archer and co-workers demonstrated a crosslinked coating design using branched thiol units, a triallyl crosslinker, fluorinated acrylate side chains and a photoinitiator[16]. In a separate study, Archer and colleagues illustrated a coating design that uses acrylate monomers crosslinked with divinylbenzene using the heat-activated radical initiator di-*tert*-butyl peroxide[15]. Wu, Zhang and collaborators demonstrated a photo-crosslinked layer of phosphoric acid 2-hydroxyethyl methacrylate ester, which effectively stabilized the PEO layer beneath it, as part of a dual-layer coating design[17].

Other than ex situ crosslinking, the in situ polymerization of small molecules in the electrolytes was also used to generate a layer of polymer coating (Fig. 2d). Huang and co-workers demonstrated the polymerization of 1,3,5-trioxane as an electrolyte additive that can be reduced by Li metal and form a layer of mechanically stable POM on the electrode surface[18]. The ring-opening polymerization of 1,3-dioxolane is also used to form a polymer layer on the Li surface, specifically for applications in solid or gel polymer electrolytes. The polymerization of 1,3-dioxolane can be triggered using aluminium triflate[58,59], tin triflate[60] and other electrophilic, nucleophilic and electron-transfer pathways[61].

In contrast to covalent bonds, non-covalent dynamic bonds can recover after rupture. In addition, the breaking of dynamic non-covalent bonds dissipates strain energy and thus increases the fracture toughness of a polymer[62]. As such, polymers with non-covalent dynamic crosslinking can achieve 'self-healing' properties, that is, the capability of recovering their original shape or mechanical strength after breakage (Fig. 2e)[63]. Examples of non-covalent dynamic bonds include hydrogen bonds and ionic bonds.

Hydrogen bonding has been used in various studies to construct mechanically robust interfaces[19,20,51]. Bao and co-workers demonstrated a coating using hydrogen bonds that resulted in more uniform Li deposition[20]. They revealed that the strength of hydrogen bonds can be fine-tuned by substituting isophorone units in the polymer chain with methylene diphenyl units (Fig. 2f). The planar atomic ring in the methylene diphenyl unit facilitates the formation of stable hydrogen bonds and increases the modulus of the polymer network. The optimal polymer composition was found to consist of 25% methylene diphenyl and 75% isophorone units, which gave the most uniform Li deposition morphology and the highest Coulombic efficiency (CE). Increasing the polymer modulus further reduced the interface's ability to adapt to the Li volumetric changes, resulting in a non-uniform Li morphology and a lower CE. The strength of the hydrogen bond can also be tuned via cooperative multivalent hydrogen bonding. For example, incorporating UPy units to the polymers enables four possible hydrogen-bonding sites to be introduced per moiety, which can increase the modulus of the material by boosting the density and strength of the hydrogen bonds[45,64].

Ionic bonds can also serve as non-covalent dynamic bonds (Fig. 2g). Wen, Guo and colleagues used Li-PAA as a self-adapting SEI[23]. Here, Li^+ can simultaneously coordinate with multiple carboxylic acid groups, forming an ionically crosslinked network. The strength of the ionic bonds can be tuned by varying the charge concentration. For example, Bao, Cui and collaborators reported a polymer network based on FTEG (that is, 1H,1H,11H,11H-perfluoro-3,6,9-trioxaundecane-1,11-diol) connected by negatively charged aluminium-oxo centres[22]. When they substituted aluminium with boron, the charge density of the $[MO_4]^-$ (M = Al, B) coordination unit increased, resulting in a higher polymer modulus. This, by contrast, decreased the coating's ability to cover the pinholes at the Li surface, which resulted in more fibrous Li deposition.

Homogenize the charge distribution

The Li deposition process has two major steps: ion transport, followed by electrochemical reduction. Maintaining an even charge distribution is crucial for achieving a uniform Li deposition[65]. Here we discuss coating designs that address the charge imbalance at the interface (both ion and electron).

Design uniform Li^+-transport pathways

In events where there is a protrusion on the electrode surface during Li plating, the negatively biased electrical field is expected to concentrate at high-curvature locations, leading to more Li^+ accumulation at these locations and preferential Li deposition (Fig. 3a)[66]. Therefore, cation-tethered polymers have been used to mitigate the potential charge-accumulation issues of the concentrated electric field. Specifically, these cations have been hypothesized to screen the negatively charged electrode surface and shield Li^+ from the concentrated electric field around surface protrusions, leading to a more uniform Li deposition morphology (Fig. 3b)[67]. Bao, Cui and co-workers designed a coating with pyrrolidinium cations tethered to an acrylic-based polymer chain, and they found that this coating led to more homogeneous Li

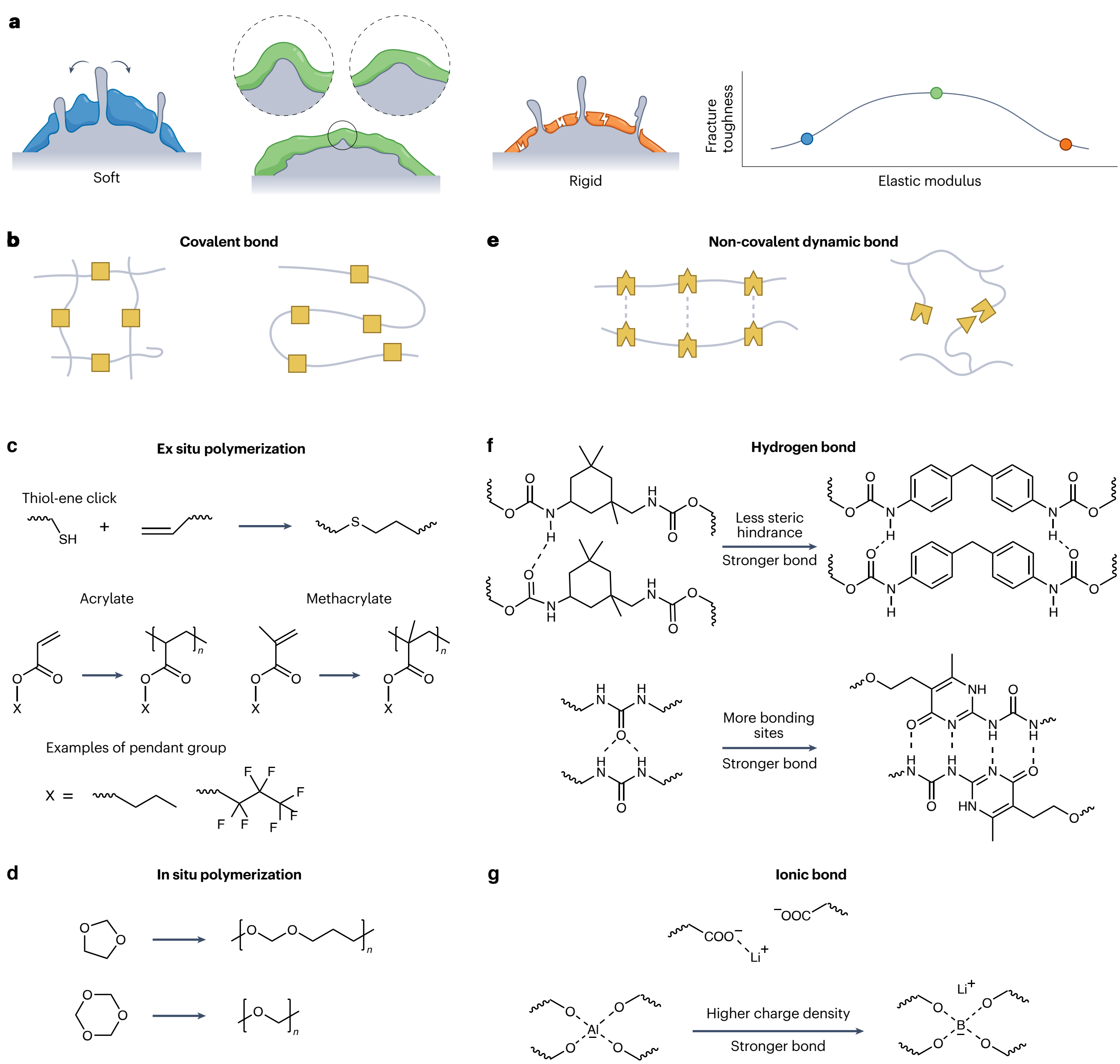

Fig. 2 | Polymer coatings aimed at maintaining coverage of the electrode surface. a, Schematic depiction of changes in Li morphology when covered with a soft (blue), rigid (orange) and high-fracture-toughness polymer layer (green). A bell curve of toughness versus modulus is shown with each of the interface scenarios marked with a dot. Circular insets (top) demonstrate the mechanism of how a high-fracture-toughness layer can maintain coverage of the Li electrode. **b**, Schematic depiction of polymer chains (in grey) connected with covalent bonds (in yellow squares). **c**, Examples of ex situ polymerization that are used to create covalent bonds[15–17]. **d**, Examples of in situ polymerization that are used to create a polymer layer on Li (refs. 18,58–61). **e**, Schematic depiction of a polymer matrix (grey) connected with dynamic bonds (yellow), which can disassociate and associate, giving different polymer network dynamics. Dynamic bonds can be periodically placed in the polymer backbone (left) or attached to polymer side chains (right). **f**, Examples of hydrogen bonds used in polymer coatings, along with how the hydrogen-bond strength can be increased by using moieties with less steric hindrance[20] (top) and higher numbers of hydrogen-bonding sites[45,64] (bottom). **g**, Examples of ionic bonds used in polymer coatings (top), along with how the ionic bond strength can be tuned with atoms of various charge densities[22,23] (bottom).

deposition and observed a doubling of the Li deposition grain size[31]. Pyrrolidinium was chosen as the cation due to its lower reduction potential than that of Li^+ and its relative stability with Li metal[68].

Alternatively, coatings may be designed that confine the Li^+ transport direction to counteract the influence of concentrated electric fields (Fig. 3c). For example, Zhu et al. reported a PDMS coating with 40–100 nm pores on Li metal[33]. They noted that increasing the pore size further led to less stable Li cycling. Helms and co-workers showed that the free volume within PIMs can regulate the flux of Li^+, where Li^+ is predominately transported through the pores in the polymer[32]. They further demonstrated that the addition of Li^+ coordination functionalities within these pores can tune the solvation environment of Li^+, which increased the Li^+ transference number from ~0.3 (baseline electrolyte) to ~0.8.

https://doi.org/10.1038/s41560-025-01767-z

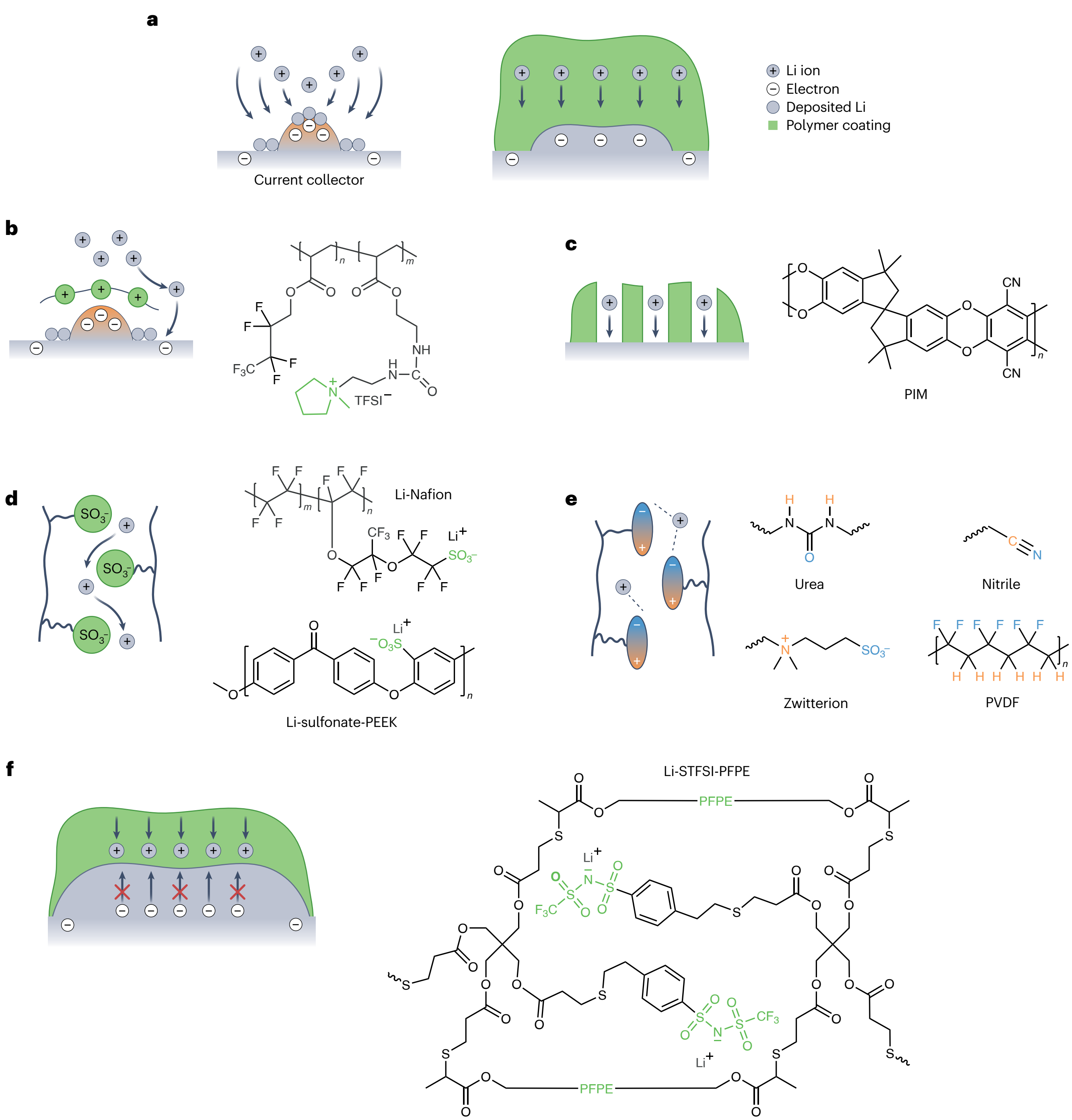

Fig. 3 | Polymer coatings can help to promote more homogeneous charge distribution at the interface. a, Schematic depictions of a concentrated electric field driving Li^+ flux towards surface protrusions during Li plating (left) and a polymer coating facilitating uniform charge distribution at the interface (right). **b**, Schematic of a polymer with tethered cations (green) shielding the concentrated electric field (left) and the structure of an example cation-containing polymer (right)[31]. **c**, Illustration of a polymer with designated ion-conduction pores regulating the Li^+ flux (left) and the structure of an example PIM polymer (right)[32,33]. **d**, Diagram of polymers with tethered sulfonate groups (green) regulating the Li^+ flux (left) and structures of example polymers Li-Nafion (top right)[29] and Li-sulfonate-PEEK (bottom right)[24]. **e**, Schematic of polymers with tethered polar groups (positive, orange; negative, blue) regulating the Li^+ flux (left) and structures of example polar groups (right): urea[33], nitrile[34], zwitterion[15] and example polymer β-phase PVDF[37]. **f**, Illustration of a polymer coating reducing the reaction kinetics but maintaining the ion-transport rate (left) and an example polymer structure with a PFPE backbone and an STFSI ion-conduction unit[42] (right).

Anionic polymers, where anions are attached within the polymer matrix, may also regulate Li^+ transport through electrostatic interactions (Fig. 3d). Archer and colleagues demonstrated a uniform Li deposition morphology using a lithiated Nafion coating, which consists of a fluorinated backbone with tethered sulfonate ($-SO_3^-$) groups[29]. Nafion selectively transports Li^+ over mobile anions, resulting in a Li transference number close to 0.9. Sulfonate groups are commonly used to introduce selective cation transport in polymers[56]. Wu, Cui and collaborators reported an ionomer interface composed of a sulfonated PEEK polymer[24]. Using operando optical microscopy, they found that this coating produced a more uniform flux of Li^+.

Polymers containing polar groups can also regulate the transport of Li^+ through polar–polar interactions with Li^+. Polar chemical functionalities typically consist of both electron-rich and electron-poor groups, forming internal dipoles, and Li^+ may interact with the electron-rich regions (Fig. 3e). These polar groups can be incorporated through chemical functionalization or the addition of inorganic compounds. For example, Cho and co-workers[41] reported a high-dielectric-constant composite polymer coating that consisted of ZrO_2 (dielectric constant = 23) and PVDF-HFP as the binder (dielectric constant = 15 (ref. 69)). They also compared Al_2O_3 and ZrO_2, and found ZrO_2 to be more effective at increasing the Li ionic conductivity and transference number, attributing this to the high dielectric constant. In addition, LiF, an electrochemically stable compound, was used as an additive in polymers such as PIM[38], PEO[39] and PVDF[40] due to its beneficial polar interactions with Li^+. Polymers with high-polarity moieties, such as PU or PAN, have been used to regulate Li^+ transport[35,36]. Another high-polarity functional group is provided by zwitterions, which contain both positive and negative charges tethered together by covalent bonds. Archer and colleagues introduced a zwitterion coating applied on Li metal using initiated chemical vapour deposition[15]. They found that the zwitterion participated in the solvation environment of Li^+, leading to a reduced exchange current density. Lastly, Wu and co-workers found that high-polarity β-phase PVDF[37], which features an all-*trans* conformation with hydrogen and fluorine atoms located on opposite sides of the polymer chain, showed promise in stabilizing the Li^+ flux. In this case, the physical separation between the electron-rich fluorine groups and the electron-poor protons created dipoles along the polymer chains.

Regulate both Li^+ transport and electron transfer

A recent study examined both the rate of ion transport and the rate of electrochemical reaction with a polymer coating (Fig. 3f). Using Brownian dynamic simulations, they revealed that a higher Li^+ transport rate compared with the reaction rate can prevent Li^+ transport from being the rate-limiting step[42], and thus reduce the need to increase the electrode surface area to disperse negative electron charges[70,71]. This results in homogeneous, low-surface-area Li deposition. This theoretical finding was realized with a coating design consisting of a PFPE polymer matrix with tethered Li-STFSI ionic groups[42]. The PFPE in the coating reduced the reaction rate at the interface by an order or magnitude while the tethered Li-STFSI enabled Li^+ transport through the polymer, maintaining the diffusivity of Li^+. The authors noted that the Li deposition morphology continued to improve as more Li-STFSI groups were incorporated into the polymer (up to 1.5 mol kg^{-1}), increasing the ionic conductivity of the polymer.

Regulate the reaction at the interface to improve SEI chemistry

Li reacts with the solvents and salts in the electrolyte, which can influence the SEI composition and morphology, and as a result the subsequent deposition of Li metal. Some studies have found that the application of a relatively inert polymer layer, such as PDMS[51] or PEO[17], may limit these reactions. Other studies seek to actively influence the SEI composition through polymer molecular design, which is explained in detail in this section.

Reactive polymer

Polymer layers can be functionalized with reactive groups to promote reactions with Li metal that improve the Li–coating adhesion or produce favourable SEI compositions (Fig. 4a). This enhanced adhesion also aids in electrolyte retention at the interface. Wang and co-workers designed a polyethylene-based polymer coating that contains cyclic ether and fluorosulfonyl groups (Fig. 4b(i),(ii))[27]. On contact with Li metal, the cyclic ether undergoes a ring-opening reaction, grafting the polymer to the Li-metal surface[46]. The fluorosulfonyl–Li reaction improved the coating's binding to the Li electrode. Xiong, Chen and colleagues reported a poly(methyl methacrylate) polymer with tethered UPy groups, designed to react with Li to increase the adhesion on the Li metal (Fig. 4b(iii))[45]. In addition, carboxylic acids were found to convert to COO^-Li^+ upon contact with Li metal (Fig. 4b(iv))[27], whereas alcohol groups were reduced (Fig. 4b(v))[47]. Fluorinated polymers such as PVDF and PVDF-HFP were found to react with Li metal and produce LiF, which is known to be a beneficial SEI component that can homogenize the Li^+ flux (Fig. 4b(vi))[43,44].

Non-reactive polymer that tunes the SEI composition

A recent report has shown the positive link between a more inorganic SEI, which is derived from salt decomposition, and the cycling stability[72]. Conversely, a solvent-derived SEI, especially from a typical carbonate-based electrolyte, has been found to be associated with poor passivation[50]. A polymer coating with selective transport of salt versus solvent may potentially tune the SEI composition (Fig. 4c).

One recent study reported the design of a polymer coating that contains both solvent-phobic (fluoroether chain; Fig. 4d) and salt-philic (ionic liquid pyrrolidinium bis(trifluoromethanesulfonyl) imide (PyTFSI); Fig. 4e) functionalities[49]. Here, the salt-philic group increased the salt–polymer interaction and the solvent-phobic group blocked the solvents. The resulting polymer increased the salt-derived SEI content and improved the cycling performance of the battery in three types of electrolyte (ether, carbonate and fluorinated ether). Other solvent-phobic moieties (for example, alkyl[49]) and salt-philic moieties (such as sulfonate[29] and urea[35]) have also been reported.

Coating–electrolyte pairs and their performances

Electrolyte engineering has been actively explored to improve the performance of LMBs[73,74]. Most polymer coatings discussed in this Review are swollen in the battery electrolyte, such that their cycling performances are also dependent on the electrolyte chemistry. In this section we examine the relationship between coating–electrolyte pairing and the overall battery performance.

Electrolyte chemistries

Most of the coating developments were examined with ether- or carbonate-based electrolytes. A typical ether-based electrolyte is composed of 1 M LiTFSI salt (lithium bis(trifluoromethanesulfonyl)imide), 1:1 v/v 1,3-dioxolane and dimethoxyethane and 1–2 wt% $LiNO_3$. The addition of the $LiNO_3$ increases the electrolyte CE from <90% to >98% (refs. 42,51). Despite the high CE, ether-based electrolytes are rarely used in full cells due to the inherent oxidative instability of ether. On the other hand, carbonate-based electrolytes have a higher oxidative stability and have been paired with high-voltage lithium nickel manganese cobalt oxide (NMC) cathodes in full-cell cycling. A typical carbonate electrolyte comprises 1 M $LiPF_6$, a solvent blend of ethylene carbonate with ethyl methyl carbonate, diethyl carbonate or dimethyl carbonate, and around 10 vol% fluoroethylene carbonate[75]. A key challenge with carbonate electrolytes is their reactivity with Li metal, which consumes both the Li metal and the electrolyte, resulting in a reduced cycle life[50].

Recently, some coatings have been paired with advanced electrolytes. One class of advanced electrolytes includes (localized) high-concentration electrolytes ((L)HCEs). Elevating the salt concentration in ether-based electrolytes is known to enhance their oxidative stability. A typical example of an HCE is 4 M lithium bis(fluorosulfonyl) imide (LiFSI) in dimethoxyethane[76]. Furthermore, the introduction of a diluent such as 1,1,2,2-tetrafluoroethyl-2,2,3,3-tetrafluoropropyl ether into the HCE was found to reduce the electrolyte viscosity and increase the ionic conductivity[72]. This electrolyte is often referred to as an 'LHCE'—a localized high-concentration electrolyte. Another class

https://doi.org/10.1038/s41560-025-01767-z

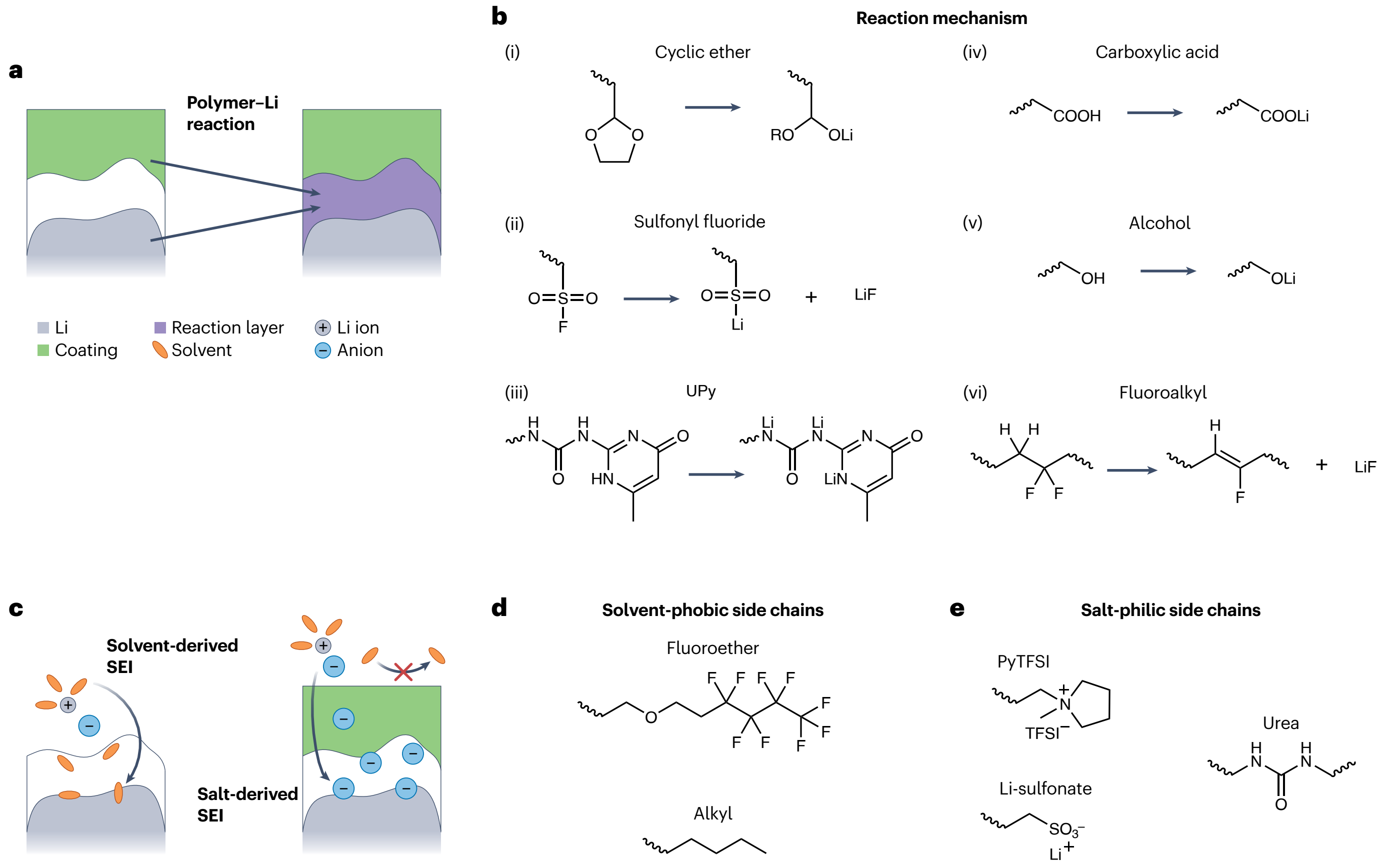

Fig. 4 | Polymer coatings that modify the reaction at the interface. a, Schematic of the reaction between a polymer and Li metal to produce an interfacial layer. **b**, Example chemical structures of functional groups that can be used in polymer coatings, and their respective reaction products from reacting with Li metal ((i)[27,46], (ii)[27], (iii)[45], (iv)[27], (v)[47] and (vi)[43,44]). **c**, Schematic of a polymer coating acting as a selective transport layer that promotes the formation of an anion-derived SEI. **d**,**e**, Example chemical structures of solvent-phobic groups[49] (**d**) and salt-philic groups[29,35,49] (**e**).

of advanced electrolyte is fluorinated ethers[77], with a typical example being 1 M LiFSI and fluorinated 1,4-dimethoxybutane (FDMB)[78] or 1.2 M LiFSI in pentafluorinated 1,2-diethoxyethane[77]. The addition of fluorine atoms on the ether molecule increases its oxidative stability, rendering it more stable for full-cell cycling. Advanced electrolytes are not limited to (L)HCEs and FDMB, and as more advanced liquid electrolytes emerge, coatings may be optimized for them[79].

Half-cell performance

In a typical Li||Cu cell, the polymer layer is coated on the Cu electrode, and ideally Li plates between the Cu electrode and the polymer coating. The 'Aurbach method'[80]—a frequently used short-term cycling protocol—consists of an activation cycle of 5 mAh cm^{-2} Li plated and stripped to 1 V versus Li$^+$/Li, followed by 5 mAh cm^{-2} plating, 10 cycles of 1 mAh cm^{-2} stripping and plating, and a final stripping step to 1 V versus Li$^+$/Li, all at the current density of 0.5 mA cm^{-2}. Here, we note the half-cell CE as CE$_{half}$, which was calculated as the ratio between all of the charges stripped and plated during the Aurbach protocols, excluding the activation cycle. For clarity in plotting, CE$_{half}$ was converted to a performance descriptor f(CE$_{half}$), which scales positively with CE$_{half}$ (ref. 81):

$$f(\mathrm{CE_{half}}) = -\log_{10}(1 - \mathrm{CE_{half}}) \quad (1)$$

Figure 5a plots the f(CE$_{half}$) data for the polymer-coated cells versus the control cells without coatings. Many examples with a coating showed an improved CE$_{half}$, as seen in the blue-shaded region. The performance of the coated cell appears to positively correlate with the performance of the underlying electrolyte (Fig. 5a), increasing roughly in the order of carbonate, ether and then advanced electrolytes ((L)HCE, FDMB). Several data points are sometimes observed from the same publication due to variations in coating composition and cycling conditions. In an ether-based electrolyte, a polysiloxane coating achieved CE$_{half}$ of 99.42%with a baseline CE$_{half}$ of 98.8% (ref. 51). The authors attributed the improved CE$_{half}$ to the chemical inertness of polysiloxane, which may reduce the tendency for chemical reaction between the electrolyte and Li metal and thus improve the SEI chemistry. The other two coatings with high CE$_{half}$ values were cycled in (L)HCE[17] and FDMB[49] electrolytes, and they both improved from the baseline CE$_{half}$ of 99.40% to 99.50%. Their notable half-cell short-term cycling performance translates to their outstanding full-cell long-term cycling, which is discussed in detail in the following section.

Full-cell performance

A typical full-cell consists of a negative Li electrode and a positive lithium iron phosphate (LFP) or NMC electrode. We attempt to capture the full-cell CE (CE$_{full}$) using the following formula:

$$(\mathrm{CE_{full}})^n = \mathrm{OCR}\,(\%) = \frac{P \times \mathrm{NCR}\,(\%)}{N + P} \quad (2)$$

Here, n is the cycle number (excluding the activation cycle); OCR is the overall capacity retention, defined as the percentage of the overall capacity remaining after the nth cycle; NCR is the nominal capacity retention, defined as the remaining percentage of the positive electrolyte capacity after the nth cycle; P is the areal capacity of the positive electrode; and N is the areal capacity of the negative electrode (Li). In this formula, the fade in capacity is attributed to the loss of active

https://doi.org/10.1038/s41560-025-01767-z

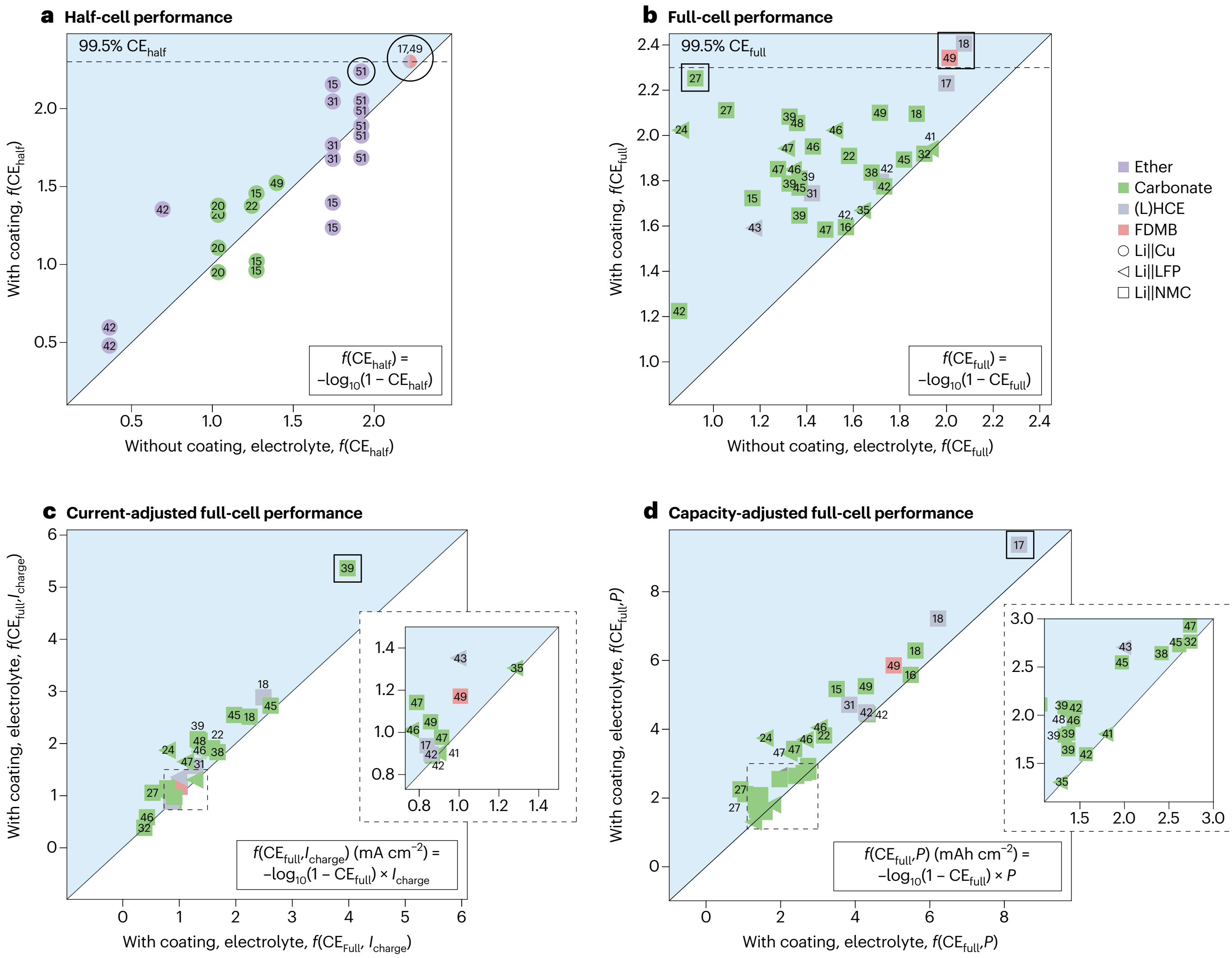

e

Reference		51	39	27	17	18	49
Electrolyte		Ether	Carbonate	Carbonate	(L)HCE	(L)HCE	FDMB
Coating composition	Polymer	Polysiloxane (PDMS)	Polyether (PEO)	Polyolefin	Polyether (PEO)	Polyether (POM)	Polysiloxane
	Additional functionality		LiF	1,3-Dioxolane, sulfonyl floride, graphene oxide	Phosphate	LiF	PyTFSI, perfluorinated alkyl
Design strategy	Maintain coverage			●	●	●	
	Homogenize charge		●		●	●	
	Improve SEI chemistry	●		●	●	●	●

Fig. 5 | Summary of coating versus electrolyte performance, accounting for the operating conditions. a–d, Parity plots comparing the performance descriptors with a polymer coating (*y* axis) and without a polymer coating (*x* axis). Performance descriptor equations are shown in each plot. As shown in the legend on the right, electrolyte types are colour-coded: ether (purple), carbonate (green), (L)HCE (grey) and fluorinated ether FDMB (red), and cell types are denoted via the symbol shapes: Li||Cu (circle), Li||LFP (triangle) and Li||NMC (square). **a**, Li||Cu half-cell performance ($f(CE_{half})$) cycled using the short-term Aurbach method. Ref. 17 is in (L)HCE and ref. 49 is in FDMB. **b**, Full-cell performance ($f(CE_{full})$) during long-term cycling. **c**, Current-adjusted full-cell performance ($f(CE_{full}, I_{charge})$) using the areal charging current density (I_{charge}). **d**, Capacity-adjusted full-cell performance ($f(CE_{full}, P)$) using the areal capacity of the positive electrode (P). In **a** and **b**, the horizontal dashed line indicates descriptor values corresponding to 99.5% CE for cells with coatings. In **c** and **d**, the insets show expansions of the data points outlined by the dashed box. In **a**–**d**, the diagonal line represents performance parity, above which (shaded in blue) cells with coatings show a higher CE than those without. The numbers inside the symbols denote the references from which the data are taken, and high-performing coating–electrolyte pairs are highlighted by the solid black borders (circles or squares). **e**, High-performing coating designs (polymer and additional functionality) for each electrolyte category, with the proposed mechanisms listed for each.

material, Li metal[82]. Under an anode-free condition (that is, $N = 0$), NCR and OCR are the same. We collected N, P and the cycle number at 80% NCR. If an 80% capacity retention was not reached, the last cycle was used. The CE_{full} value was converted to a performance descriptor $f(CE_{full})$, which scales positively with CE_{full} (ref. 81):

$$f(CE_{full}) = -\log_{10}(1 - CE_{full}) \quad (3)$$

Figure 5b shows the full-cell performance of polymer-coated cells versus control cells without coatings. We examine the three cells with the top $f(CE_{full})$ values.

Wang and co-workers developed a reactive coating[27] for a carbonate electrolyte that achieved a CE_{full} of 99.44%, cycled at an N-to-P ratio of 24, a C-rate of C/2 and with an electrolyte amount of 12 µl mAh^{-1}. The coating was designed to react with Li metal to improve the SEI chemistry. It comprises polyolefin with reactive side chains (that is, 1,3-dioxolane and sulfonyl fluoride) and carboxylic acid-functionalized graphene oxide. It was hypothesized that the improved lean electrolyte cycling was due to the coating's improved electrolyte retention at the interface.

Bao, Cui and colleagues developed a polysiloxane-based coating[49] for the FDMB electrolyte, demonstrating a CE_{full} of 99.55% at $N/P = 4$, $P = 2.5$ mAh cm^{-2}, C/5 charge and discharge and an electrolyte amount of 16 µl mAh^{-1}. The polymer, named SP^2, contains both salt-philic (PyTFSI) and solvent-phobic (perfluorinated alkyl) moieties that promoted salt-derived SEI formation and improved the SEI chemistry[77].

Huang and co-workers developed a polyether (POM)-based interface[18] for the (L)HCE electrolyte, demonstrating a CE_{full} of 99.61% at $N/P = 3.3$, $P = 3$ mAh cm^{-2}, 0.4C charge and discharge and an electrolyte amount of 17 µl mAh^{-1}. This work demonstrated the co-designing of an electrolyte and coating pair: the proposed dual-layer interface is composed of a F-rich anion-derived bottom layer from (L)HCE decomposition and a top POM layer from the ring-opening polymerization of 1,3,5-trioxane. The electrolyte decomposition contributes to improved SEI chemistry and homogeneity at the interface, while the polymer layer enhances the mechanical stability of the SEI.

The full-cell performance was also compared upon factoring in the current and capacity conditions during cycling. Figure 5c shows the current-adjusted full-cell performance as the descriptor $f(CE_{full}, I_{charge})$. The charging density (measured in mA cm^{-2}) is used for its relevance in Li deposition.

$$f(CE_{full}, I_{charge}) = -\log_{10}(1 - CE_{full}) \times I_{charge} \quad (4)$$

Nine of the top ten $f(CE_{full}, I_{charge})$ values were demonstrated in carbonate electrolytes, showing the carbonate electrolyte's ability to cycle at a high current density. The highest $f(CE_{full}, I_{charge})$ represents a CE_{full} of 98.37% at 3 mA cm^{-2} ($N/P = 50$, $P = 1$ mAh cm^{-2}, electrolyte amount = 30 µl mAh^{-1}), with a PEO and LiF composite coating developed by Fu and Battaglia[39]. After swelling in the carbonate electrolyte, this coating achieved a conductivity of 0.97 mS cm^{-1} with a Li^+ transference number of 0.77, and was proposed to homogenize charge distribution at the interface.

Figure 5d shows the capacity-adjusted full-cell performance with the descriptor $f(CE_{full}, P)$, using the areal capacity of the positive electrode (in mAh cm^{-2}):

$$f(CE_{full}, P) = -\log_{10}(1 - CE_{full}) \times P \quad (5)$$

Two of the top three $f(CE_{full}, P)$ values were demonstrated in either (L)HCE or FDMB, showing the stability of the advanced electrolytes with Li metal, enabling high-capacity cycling. The highest $f(CE_{full}, P)$ was cycled at 4.2 mAh cm^{-2} in (L)HCE with a CE_{full} of 99.41% ($N/P = 2.4$, C-rate = C/2, electrolyte amount = 16 µl mAh^{-1}), with a dual-layer PEO-based coating developed by Wu, Zhang and collaborators[17]. This coating comprises of a base layer of PEO and a top layer of crosslinked phosphate polymer. The PEO layer improved the SEI chemistry by suppressing the Li–solvent reaction and homogenizing the Li^+ flux. The crosslinked phosphate layer prevented the dissolution of PEO and maintained its coverage of the electrode.

Trends among high-performing designs

Figure 5e summarizes the six aforementioned high-performing coating–electrolyte pairs, with details shown for their coating chemistry and design strategies. There are key trends among these designs. First, pairing with advanced electrolytes leads to a high CE during both half-cell and full-cell cycling, and the top two designs originated from coatings that were paired with advanced electrolytes. Second, polyether and polysiloxane exhibit key polymer chemistries, as coatings that used either polyether or polysiloxane chemistries achieved the highest CE values during half-cell[17,49] and full-cell[18,49] cycling, showing the chemical stability of these polymers. In addition, the two coatings that demonstrated the highest current-adjusted[39] and capacity-adjusted[17] performances both used polyether (PEO) chemistry, highlighting the ability of the ether oxygen to maintain ion conduction. Third, additional coating functionalities often involve an anion-derived SEI. The SEI derived from anion breakdown instead of solvent breakdown has been linked to an improved LMB performance[72]. Components from an anion-derived SEI (for example, LiF) can be incorporated as part of the composites[18,39]. Alternatively, anion-derived SEI formation can be engineered with reactive coatings[27] or coatings that reduce solvent decomposition[49]. Last, improving the SEI chemistry is the key design strategy: five of the six highlighted coating–electrolyte pairs proposed improving the SEI chemistry as one of the design strategies. This includes using polymer chemistries that are relatively inert with Li metal (for example, PEO[17] and polysiloxane[51]), engineering chemical reactions at the interface[27,49] or co-designing with an electrolyte that is known for improved SEI chemistry[18]. Other mechanisms, such as maintaining coverage and homogenizing the charge distribution, remain important considerations and are basic requirements for the stable long-term operation of the coating.

Outlook

Opportunities for improvement

New opportunities for LMB performance improvement have emerged through the consideration of realistic cycling conditions and from recent understandings of the battery failure mechanism. Regarding current density, coating–carbonate electrolyte combinations have achieved some of the highest reported cycling current densities, despite the reactive nature of carbonates. Polymer coatings that suppress the reactivity of the carbonate electrolyte may provide a pathway for both a high CE and high-current-density cycling. Regarding resting, Li-metal corrosion and SEI dissolution during battery resting contribute to capacity fading. Coatings with low dielectric constants could enhance active Li preservation and minimize corrosion during the rest period. Regarding electrode crosstalk, the leakage of transition metals from the positive to the negative electrode has been identified as a mechanism that contributes to capacity fading in Li batteries[83]. Designing polymer materials that limit transition metal transport may suppress electrode crosstalk and prolong the cycle life.

Considerations for co-designing with emerging electrolytes

As more promising liquid electrolytes emerge[79,84], designing polymer coatings in combination with specific electrolytes may be the next step for further boosting the performance of LMBs. First, the functions of many novel electrolytes rely on their unique solvation structures with Li^+. The role of polymer coatings in altering the solvation structure at the interface should be carefully examined. Second, the effect of coatings on the SEI chemistry may not undercut the electrolyte's inherent benefit for the Li-metal stability. Third, the properties of coatings under electrolyte-induced swelling should be examined, as swelling affects mechanical strength, ionic conductivity, Li^+ transference and chemical reactivity. Last, the contribution of the coating to the interfacial mechanics and ion conduction depends on its thickness, which can be optimized to maximize the benefit delivered by the coating[16,51].

Summary

In this Review, we discuss the design of polymer coatings and their roles in stabilizing Li metal through three key mechanisms: maintaining coverage, homogenizing the charge distribution and improving the SEI chemistry. For each mechanism, we explore relevant polymer backbone and functional group chemistries. We review both the short-term and long-term cycling performance of cells with polymer coatings and find that improving the SEI chemistry may be a promising design strategy towards high-performing LMBs. Finally, we pinpoint the opportunities and considerations for designing coatings with emerging electrolyte systems.

References

1. Liu, J. et al. Pathways for practical high-energy long-cycling lithium metal batteries. *Nat. Energy* **4**, 180–186 (2019).
This paper proposed practical guidelines for the characterization of LMBs.
2. Whittingham, M. History, evolution, and future status of energy storage. *Proc. IEEE* **100**, 1518–1534 (2012).
3. Tikekar, M. D., Choudhury, S., Tu, Z. & Archer, L. A. Design principles for electrolytes and interfaces for stable lithium-metal batteries. *Nat. Energy* **1**, 16114 (2016).
This paper highlights challenges related to the instability of Li-metal anodes.
4. Gong, H. et al. Fast-charging of hybrid lithium-ion/lithium-metal anodes by nanostructured hard carbon host. *ACS Energy Lett.* **7**, 4417–4426 (2022).
5. Yan, K. et al. Selective deposition and stable encapsulation of lithium through heterogeneous seeded growth. *Nat. Energy* **1**, 16010 (2016).
6. Xu, R. et al. Artificial interphases for highly stable lithium metal anode. *Matter* **1**, 317–344 (2019).
7. Yan, C. et al. Dual-layered film protected lithium metal anode to enable dendrite-free lithium deposition. *Adv. Mater.* **30**, 1707629 (2018).
8. Sun, S. et al. Facile ex situ formation of a LiF–polymer composite layer as an artificial SEI layer on Li metal by simple roll-press processing for carbonate electrolyte-based Li metal batteries. *J. Mater. Chem. A* **8**, 17229–17237 (2020).
9. Basile, A., Bhatt, A. I. & O'Mullane, A. P. Stabilizing lithium metal using ionic liquids for long-lived batteries. *Nat. Commun.* **7**, ncomms11794 (2016).
10. Zheng, G. et al. Interconnected hollow carbon nanospheres for stable lithium metal anodes. *Nat. Nanotechnol.* **9**, 618–623 (2014).
11. Chen, L. et al. Lithium metal protected by atomic layer deposition metal oxide for high performance anodes. *J. Mater. Chem. A* **5**, 12297–12309 (2017).
12. Chen, L. et al. Directly formed alucone on lithium metal for high-performance Li batteries and Li–S batteries with high sulfur mass loading. *ACS Appl. Mater. Interfaces* **10**, 7043–7051 (2018).
13. Zhou, H., Yu, S., Liu, H. & Liu, P. Protective coatings for lithium metal anodes: recent progress and future perspectives. *J. Power Sources* **450**, 227632 (2020).
14. Lin, D., Liu, Y. & Cui, Y. Reviving the lithium metal anode for high-energy batteries. *Nat. Nanotechnol.* **12**, 194–206 (2017).
15. Stalin, S. et al. Ultrathin zwitterionic polymeric interphases for stable lithium metal anodes. *Matter* **4**, 3753–3773 (2021).
16. Stalin, S. et al. Designing polymeric interphases for stable lithium metal deposition. *Nano Lett.* **20**, 5749–5758 (2020).
17. Kim, J.-M. et al. High current-density-charging lithium metal batteries enabled by double-layer protected lithium metal anode. *Adv. Funct. Mater.* **32**, 2207172 (2022).
18. Zhang, Q.-K. et al. Homogeneous and mechanically stable solid–electrolyte interphase enabled by trioxane-modulated electrolytes for lithium metal batteries. *Nat. Energy* **8**, 725–735 (2023).
19. Zheng, G. et al. High-performance lithium metal negative electrode with a soft and flowable polymer coating. *ACS Energy Lett.* **1**, 1247–1255 (2016).
20. Huang, Z. et al. Effects of polymer coating mechanics at solid–electrolyte interphase for stabilizing lithium metal anodes. *Adv. Energy Mater.* **12**, 2103187 (2022).
21. Liu, K. et al. Lithium metal anodes with an adaptive "solid-liquid" interfacial protective layer. *J. Am. Chem. Soc.* **139**, 4815–4820 (2017).
22. Yu, Z. et al. A dynamic, electrolyte-blocking, and single-ion-conductive network for stable lithium-metal anodes. *Joule* **3**, 2761–2776 (2019).
23. Li, N.-W. et al. A flexible solid electrolyte interphase layer for long-life lithium metal anodes. *Angew. Chem. Int. Ed.* **57**, 1505–1509 (2018).
24. Weng, Y.-T. et al. An ultrathin ionomer interphase for high efficiency lithium anode in carbonate based electrolyte. *Nat. Commun.* **10**, 5824 (2019).
25. Liu, F. et al. Fabrication of hybrid silicate coatings by a simple vapor deposition method for lithium metal anodes. *Adv. Energy Mater.* **8**, 1701744 (2018).
26. Xu, R. et al. Artificial soft–rigid protective layer for dendrite-free lithium metal anode. *Adv. Funct. Mater.* **28**, 1705838 (2018).
27. Gao, Y. et al. Polymer–inorganic solid–electrolyte interphase for stable lithium metal batteries under lean electrolyte conditions. *Nat. Mater.* **18**, 384–389 (2019).
28. Zhao, Y. et al. Natural SEI-inspired dual-protective layers via atomic/molecular layer deposition for long-life metallic lithium anode. *Matter* **1**, 1215–1231 (2019).
29. Tu, Z. et al. Designing artificial solid–electrolyte interphases for single-ion and high-efficiency transport in batteries. *Joule* **1**, 394–406 (2017).
30. Kozen, A. C. et al. Stabilization of lithium metal anodes by hybrid artificial solid electrolyte interphase. *Chem. Mater.* **29**, 6298–6307 (2017).
31. Huang, Z., Choudhury, S., Gong, H., Cui, Y. & Bao, Z. A cation-tethered flowable polymeric interface for enabling stable deposition of metallic lithium. *J. Am. Chem. Soc.* **142**, 21393–21403 (2020).
32. Baran, M. J. et al. Diversity-oriented synthesis of polymer membranes with ion solvation cages. *Nature* **592**, 225–231 (2021).
33. Zhu, B. et al. Poly(dimethylsiloxane) thin film as a stable interfacial layer for high-performance lithium-metal battery anodes. *Adv. Mater.* **29**, 1603755 (2017).
34. Liu, Y. et al. An artificial solid electrolyte interphase with high Li-ion conductivity, mechanical strength, and flexibility for stable lithium metal anodes. *Adv. Mater.* **29**, 1605531 (2017).
35. Sun, Y. et al. A novel organic "polyurea" thin film for ultralong-life lithium-metal anodes via molecular-layer deposition. *Adv. Mater.* **31**, 1806541 (2019).
36. Zhou, H. et al. Quantification of the ion transport mechanism in protective polymer coatings on lithium metal anodes. *Chem. Sci.* **12**, 7023–7032 (2021).
37. Luo, J., Fang, C.-C. & Wu, N.-L. High polarity poly(vinylidene difluoride) thin coating for dendrite-free and high-performance lithium metal anodes. *Adv. Energy Mater.* **8**, 1701482 (2018).
38. Fu, C. et al. Universal chemomechanical design rules for solid-ion conductors to prevent dendrite formation in lithium metal batteries. *Nat. Mater.* **19**, 758–766 (2020).

39. Fu, C. & Battaglia, C. Polymer–inorganic nanocomposite coating with high ionic conductivity and transference number for a stable lithium metal anode. *ACS Appl. Mater. Interfaces* **12**, 41620–41626 (2020).
40. Liu, H.-J. et al. Engineering lithiophilic silver sponge integrated with ion-conductive PVDF/LiF protective layer for dendrite-free and high-performance lithium metal batteries. *ACS Appl. Energy Mater.* **6**, 519–529 (2023).
41. Jang, E. K., Ahn, J., Yoon, S. & Cho, K. Y. High dielectric, robust composite protective layer for dendrite-free and $LiPF_6$ degradation-free lithium metal anode. *Adv. Funct. Mater.* **29**, 1905078 (2019).
42. Choudhury, S. et al. Ion conducting polymer interfaces for lithium metal anodes: impact on the electrodeposition kinetics. *Adv. Energy Mater.* **13**, 2301899 (2023).
43. Guo, Q. et al. CNT/PVDF composite coating layer on Cu with a synergy of uniform current distribution and stress releasing for improving reversible Li plating/stripping. *ACS Appl. Mater. Interfaces* **14**, 46043–46055 (2022).
44. Guo, S. et al. PVDF-HFP/LiF composite interfacial film to enhance the stability of Li-metal anodes. *ACS Appl. Energy Mater.* **3**, 7191–7199 (2020).
45. Wang, G. et al. Self-stabilized and strongly adhesive supramolecular polymer protective layer enables ultrahigh-rate and large-capacity lithium-metal anode. *Angew. Chem. Int. Ed.* **59**, 2055–2060 (2020).
46. Gao, Y. et al. Interfacial chemistry regulation via a skin-grafting strategy enables high-performance lithium-metal batteries. *J. Am. Chem. Soc.* **139**, 15288–15291 (2017).
47. Zhao, Y. et al. Stable Li metal anode by a polyvinyl alcohol protection layer via modifying solid–electrolyte interphase layer. *Nano Energy* **64**, 103893 (2019).
48. Liu, Y. et al. Solubility-mediated sustained release enabling nitrate additive in carbonate electrolytes for stable lithium metal anode. *Nat. Commun.* **9**, 3656 (2018).
49. Huang, Z. et al. A salt-philic, solvent-phobic interfacial coating design for lithium metal electrodes. *Nat. Energy* **8**, 577–585 (2023).
50. Aurbach, D., Zinigrad, E., Cohen, Y. & Teller, H. A short review of failure mechanisms of lithium metal and lithiated graphite anodes in liquid electrolyte solutions. *Solid State Ion.* **148**, 405–416 (2002).
51. Lopez, J. et al. Effects of polymer coatings on electrodeposited lithium metal. *J. Am. Chem. Soc.* **140**, 11735–11744 (2018).
52. Monroe, C. & Newman, J. The impact of elastic deformation on deposition kinetics at lithium/polymer interfaces. *J. Electrochem. Soc.* **152**, A396 (2005).
This work links the Li deposition morphology to interfacial mechanical properties.
53. Cao, D. et al. Lithium dendrite in all-solid-state batteries: growth mechanisms, suppression strategies, and characterizations. *Matter* **3**, 57–94 (2020).
54. Kong, X., Rudnicki, P. E., Choudhury, S., Bao, Z. & Qin, J. Dendrite suppression by a polymer coating: a coarse-grained molecular study. *Adv. Funct. Mater.* **30**, 1910138 (2020).
55. Khurana, R., Schaefer, J. L., Archer, L. A. & Coates, G. W. Suppression of lithium dendrite growth using cross-linked polyethylene/poly(ethylene oxide) electrolytes: a new approach for practical lithium-metal polymer batteries. *J. Am. Chem. Soc.* **136**, 7395–7402 (2014).
56. Hallinan, D. T. Jr & Balsara, N. P. Polymer electrolytes. *Annu. Rev. Mater. Res.* **43**, 503–525 (2013).
57. Mavila, S., Eivgi, O., Berkovich, I. & Lemcoff, N. G. Intramolecular cross-linking methodologies for the synthesis of polymer nanoparticles. *Chem. Rev.* **116**, 878–961 (2016).
58. Utomo, N. W. et al. Solid-state polymer–particle hybrid electrolytes: structure and electrochemical properties. *Sci. Adv.* **10**, eado4719 (2024).
59. Zhao, Q., Liu, X., Stalin, S., Khan, K. & Archer, L. A. Solid-state polymer electrolytes with in-built fast interfacial transport for secondary lithium batteries. *Nat. Energy* **4**, 365–373 (2019).
60. Zheng, J. et al. In-situ polymerization with dual-function electrolyte additive toward future lithium metal batteries. *Mater. Today Energy* **26**, 100984 (2022).
61. Aurbach, D., Youngman, O. & Dan, P. The electrochemical behavior of 1,3-dioxolane–$LiClO_4$ solutions—II. Contaminated solutions. *Electrochim. Acta* **35**, 639–655 (1990).
62. Wojtecki, R. J., Meador, M. A. & Rowan, S. J. Using the dynamic bond to access macroscopically responsive structurally dynamic polymers. *Nat. Mater.* **10**, 14–27 (2011).
63. Stukalin, E. B., Cai, L.-H., Kumar, N. A., Leibler, L. & Rubinstein, M. Self-healing of unentangled polymer networks with reversible bonds. *Macromolecules* **46**, 7525–7541 (2013).
64. Mackanic, D. G. et al. Decoupling of mechanical properties and ionic conductivity in supramolecular lithium ion conductors. *Nat. Commun.* **10**, 5384 (2019).
65. Bai, P., Li, J., Brushett, F. R. & Bazant, M. Z. Transition of lithium growth mechanisms in liquid electrolytes. *Energy Environ. Sci.* **9**, 3221–3229 (2016).
66. Chazalviel, J.-N. Electrochemical aspects of the generation of ramified metallic electrodeposits. *Phys. Rev. A* **42**, 7355–7367 (1990).
This work describes how charge imbalance leads to heterogeneous metal deposition.
67. Ding, F. et al. Dendrite-free lithium deposition via self-healing electrostatic shield mechanism. *J. Am. Chem. Soc.* **135**, 4450–4456 (2013).
68. Wang, X. et al. Poly(ionic liquid)s-in-salt electrolytes with co-coordination-assisted lithium-ion transport for safe batteries. *Joule* **3**, 2687–2702 (2019).
69. Zhou, X. et al. Electrical breakdown and ultrahigh electrical energy density in poly(vinylidene fluoride–hexafluoropropylene) copolymer. *Appl. Phys. Lett.* **94**, 162901 (2009).
70. Liu, Y. et al. Insight into the critical role of exchange current density on electrodeposition behavior of lithium metal. *Adv. Sci.* **8**, 2003301 (2021).
71. Boyle, D. T. et al. Correlating kinetics to cyclability reveals thermodynamic origin of lithium anode morphology in liquid electrolytes. *J. Am. Chem. Soc.* **144**, 20717–20725 (2022).
72. Ren, X. et al. Localized high-concentration sulfone electrolytes for high-efficiency lithium-metal batteries. *Chem* **4**, 1877–1892 (2018).
73. Xu, K. Nonaqueous liquid electrolytes for lithium-based rechargeable batteries. *Chem. Rev.* **104**, 4303–4418 (2004).
This work summarizes common salts and solvents for Li batteries.
74. Wang, H. et al. Liquid electrolyte: the nexus of practical lithium metal batteries. *Joule* **6**, 588–616 (2022).
75. Etacheri, V. et al. Effect of fluoroethylene carbonate (FEC) on the performance and surface chemistry of Si-nanowire Li-ion battery anodes. *Langmuir* **28**, 965–976 (2012).
76. Qian, J. et al. High rate and stable cycling of lithium metal anode. *Nat. Commun.* **6**, 6362 (2015).
77. Yu, Z. et al. Rational solvent molecule tuning for high-performance lithium metal battery electrolytes. *Nat. Energy* **7**, 94–106 (2022).
78. Yu, Z. et al. Molecular design for electrolyte solvents enabling energy-dense and long-cycling lithium metal batteries. *Nat. Energy* **5**, 526–533 (2020).

79. Hobold, G. M. et al. Moving beyond 99.9% Coulombic efficiency for lithium anodes in liquid electrolytes. *Nat. Energy* **6**, 951–960 (2021).
80. Adams, B. D., Zheng, J., Ren, X., Xu, W. & Zhang, J.-G. Accurate determination of Coulombic efficiency for lithium metal anodes and lithium metal batteries. *Adv. Energy Mater.* **8**, 1702097 (2018).
81. Kim, S. C. et al. Data-driven electrolyte design for lithium metal anodes. *Proc. Natl Acad. Sci. USA* **120**, e2214357120 (2023).
82. Xiao, J. et al. Understanding and applying coulombic efficiency in lithium metal batteries. *Nat. Energy* **5**, 561–568 (2020).
83. Song, Y. et al. The significance of imperceptible crosstalk in high-energy batteries. *Energy Storage Mater.* **63**, 103018 (2023).
84. Meng, Y. S., Srinivasan, V. & Xu, K. Designing better electrolytes. *Science* **378**, eabq3750 (2022).

Acknowledgements

The authors acknowledge support from the Assistant Secretary for Energy Efficiency and Renewable Energy (EERE), Office of Vehicle Technologies (VTO) of the US Department of Energy (DOE) under the Battery Materials Research (BMR) Program and Battery 500 Consortium.

Author contributions

All authors contributed to the writing and revision of the manuscript.

Competing interests

The authors declare no competing interests.

Additional information

Correspondence and requests for materials should be addressed to Yi Cui or Zhenan Bao.

Peer review information *Nature Energy* thanks Jia-Qi Huang, Wei-Hong Lai and the other, anonymous, reviewer for their contribution to the peer review of this work.